

Sequence Impedance of Submarine Cables

**Thomas KVARTS*,
Anna Candela GAROLERA, Ziyi HUANG
ØRSTED
Denmark
thokv@orsted.com**

**Ola THYRVIN*
NKT HV CABLES AB
Sweden
ola.thyrvin@nkt.com**

SUMMARY

CIGRE Technical Brochure 531 is widely referenced for high voltage a.c. cable circuit sequence impedance calculation in the cable industry. Although it provides quick and reliable results for underground cable system(s), it has certain intrinsic shortcomings for modern 3-core submarine cable system(s) due to assumptions and simplifications adopted in deriving the final analytical formulae. In general, the calculation accuracy of the simplified analytical formulae also becomes less reliable for higher frequencies (up to the 50th - 100th harmonics required for power system studies today). In order to improve the calculation accuracy and reliability, offshore windfarm developer Ørsted has collaborated with cable supplier NKT to develop new analytical sequence impedance calculation methods for modern 3-core submarine cable system(s). The method presented in this paper is based on first principles, classic circuit theory, and existing industrial cable design best practice, and has been developed in such a way to retain an analytical form. The base credibility and accuracy of the developed method is examined through calculation comparison against alternative numerical method(s). Finally, considering its analytical nature which inevitably involves certain simplifications, a step-by-step calculation demonstration is prepared, and supplementary guidelines/ recommendations are provided to clarify its applicability against various cable designs and operation conditions.

KEYWORDS

HVAC, 3-core Submarine Cable, Sequence Impedance, Analytical Calculation, Carson

1. Introduction

For large-scale HVAC power system design and operation, the sequence impedance characteristics of system equipment/ assets are important design parameters which could greatly influence the system power flow study and system fault analysis.

Considering the increasing number of HVAC connected offshore windfarm developments with longer to-shore distances, the amount of submarine cables needed to facilitate these connections increases sharply and accurate sequence impedance calculations for the cable assets become critical.

However, it has been observed that the calculated sequence impedance values from different suppliers deviate significantly from each other even for a similar submarine cable design with supposedly simple designs with non-magnetic armour. It results in greater uncertainties about the value credibility; therefore, larger design contingency has to be included leading to higher project costs. One possible cause for this unpleasant situation is the lack of a widely agreed calculation methodology specific for modern submarine cable systems. Although CIGRE Technical Brochure (TB) 531 ‘Cable Systems Electrical Characteristics’ [1] proposes simplified analytical formulae, it is better addressed for underground cable systems while a number of improvements are still needed for submarine cables to meet the accuracy requirements of modern submarine cable connections.

Therefore, this paper presents an improved analytical calculation methodology based on first principles, classic circuit theory, and existing industrial cable design best practice (e.g. IEC 60287-1-1 [2] formulae), taking into account practical offshore windfarm development & operation experience. It is intended to be a first attempt of aiding the industry to a common approach, but it is recommended to followed up by a CIGRE work group to update CIGRE TB531 on the matter of submarine cables.

1.1 Knowledge gap and challenges

When applying Cigre TB 531 sequence impedance calculations for modern 3-core submarine cable circuits, several challenges are observed without an unambiguous guidance for addressing them.

- Insufficient applicability/ accuracy of the simplified analytical positive sequence impedance formula for higher frequencies (up to the 50th to 100th harmonic often requested for stability studies);
- Simplified analytical zero sequence impedance formula has excluded cable armour layer as parallel earth return path, which could undermine the resulting credibility and accuracy;
- Influence of magnetic armour on the submarine cable component electrical parameter calculation seems overly simplified;
- No instruction to include skin effect and proximity effect from the rating calculations of IEC 60287 in the a.c. resistance impedance of the conductor;
- No inclusion of eddy currents now recommended to be included in load calculations by CIGRE WG B1.56 [3]; and
- No discussion on the inclusion of the lay factor of the core assembly or armour.

Although several comprehensive matrix based numerical calculation methodologies are introduced in TB 531 Appendices, which could potentially address the above-mentioned shortcomings, unfortunately, a straight-forward application guidance is not included, which makes it very hard to implement in practice.

In literature it has also been hard to find well worked guidance, that is not rooted in studies for very high frequency transients (thus including Bessel functions) or very simplified solutions not coupling the knowledge from the load calculations of IEC 60287 of SL type cables with transmission line modelling.

1.2 Paper structure

This paper will present two methodologies widely quoted calculation in the industry, that are reviewed with discussion of both pros and cons when applied to modern submarine cables; and subsequently, the newly proposed analytical calculation method is introduced followed by a step-by-step application demonstration with results benchmarking. Finally, the applicability of the new method is discussed, and potential future developments are outlined to enhance its applicability and accuracy.

2. Calculation Method

For most cable suppliers, a simplified analytical calculation method is preferred. However, there is no clear industrial consensus for submarine cable sequence impedance calculation and various analytical methods have been used [1] [4] [5]. In addition, certain suppliers who realise the limitations of existing analytical methods thus adopt more advanced calculations such as complex impedance matrix (CIM) and finite element analysis (FEA).

2.1 Existing methods widely used

2.1.1 Cigre TB 531

The Cigre TB 531 presents both a simplified analytical methodology and a comprehensive numerical methodology to calculate the positive/ negative and zero sequence impedances of submarine three-core cables. For the sake of easy-to-handle formulae for most cases, the analytical methodology includes large simplifications and applies only to power frequency.

Within the simplified analytical methodology, the positive/ negative sequence impedance, referred to in [1] as Z_d , corresponds to the ratio of the normal power frequency voltage along the cable to the three-phase current on the cable conductors and the zero impedance, referred to in [1] as Z_h , corresponds to the ratio of the voltage along the cable to a current equal in magnitude and phase on the three cable conductors, where the current returns through the metal screens and the surrounding earth. The associated formulae are reproduced below, and all associated parameters are well defined in [1].

$$Z_d = (Z_a - Z_x) - \frac{(Z_m - Z_x)^2}{Z_s - Z_x} + R_a \cdot \lambda_2 \quad (1)$$

$$Z_h = R' \cdot (1 + Y_s) + j \cdot X_a + 2 \cdot Z_x - \frac{(Z_m - 2 \cdot Z_x)^2}{Z_s - 2 \cdot Z_x} \quad (2)$$

The self and mutual impedances of the cable conductors and screens used in Equ. (1) and Equ. (2) are calculated considering that the current flowing in the phase conductors returns through the surrounding earth. The surrounding earth is modelled as an equivalent conductor with a resistance R'_E and an equivalent depth D_E , but that the factor \sqrt{e} is “missing” in the numerator in Equ. (4) for offshore cables in an infinite medium (the seabed and the sea) compared to onshore [1] [6] [7] which is often overlooked.

$$R'_E = \frac{\omega \cdot \mu_0}{8} \quad (3)$$

$$D_E = \frac{2}{\gamma_b \sqrt{g_s \omega \mu}} = 400 \sqrt{\frac{\rho}{f}} \quad (4)$$

As described in Section 1.1, this methodology does not include the cable armour as a parallel current return path. This may lead to significant deviations in the zero sequence impedance compared with other calculation methods that include the armour return path.

2.1.2 Complex impedance matrix

One way to set up the complex impedance matrix (CMI), reduce it according to Z_0 if matrix calculations are available, is to set up the full Z matrix for all conductors with the same approximate Carson's formulas with earth return. The method is described to some degree in Cigre TB 531 [1] Appendix B.7 but not for submarine cables, and a more descriptive formulation can be found in [8]. Here we will set up the incident node matrix to reduce the impedance matrix.

The advantage is that the model is set up once and can be expanded to other geometries and additional ground returns or systems can be added with the same basic setup. It however requires a tool with matrix calculation capability.

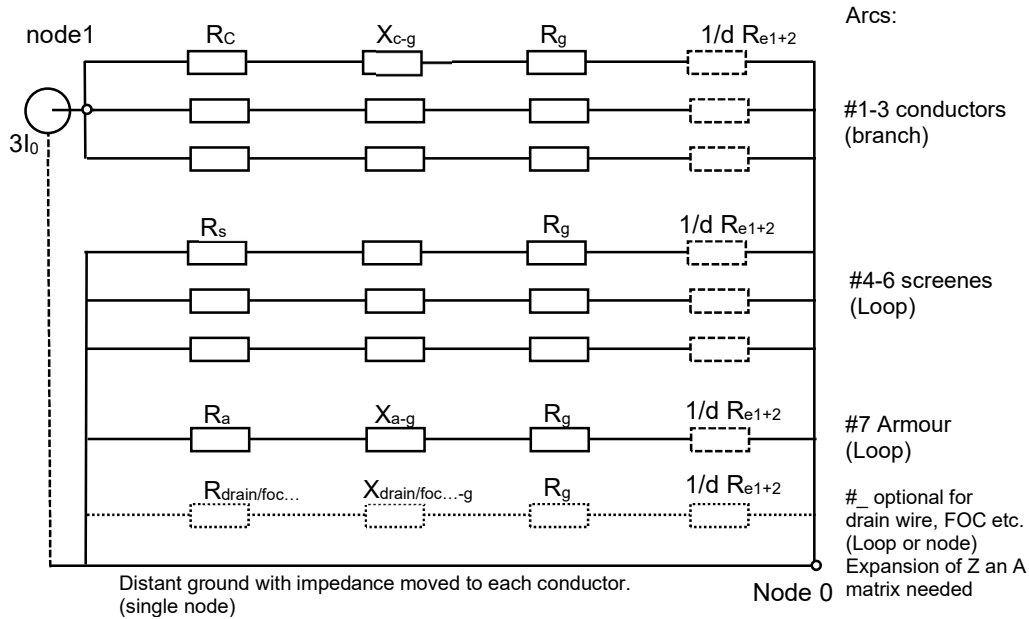


Figure 1 – Circuit topology for creating the incident matrix for the CIM method

First, the impedance matrix is set up by simplified Carson's solutions with all inductances referenced to earth return. This is done based on the x and y coordinate vectors (XX , YY) of all conductors, 3 conductors, 3 screens and the armour. More rows could be added for internal drain wires, Fibre optical cables, etc.

Taking the 3-core submarine cable design from case 8 of Cigre WG B1.56 study (in final draft at the time of writing) [3] as an example, the Geometrical Mean Distance GMD matrix is built from the X/Y vectors for centre position of metallic conductors. For offshore cables earth connections at the extremities are of often very low resistance (offshore steel platforms or transition joint bays with earth grid connected to the armour of the cable) and armour and most sheaths are continuously grounded so R_e is neglected.

$XX := \begin{pmatrix} 0 \\ -c \cdot \cos\left(\frac{\pi}{6}\right) \\ -c \cdot \cos\left(\frac{\pi}{6}\right) \\ 0 \\ -c \cdot \cos\left(\frac{\pi}{6}\right) \\ -c \cdot \cos\left(\frac{\pi}{6}\right) \\ 0 \end{pmatrix} = \begin{pmatrix} 0 \\ 52.3 \\ -52.3 \\ 0 \\ 52.3 \\ -52.3 \\ 0 \end{pmatrix} \cdot \text{mm}$ $YY := \begin{pmatrix} -c \\ -c \cdot \sin\left(\frac{\pi}{6}\right) \\ -c \cdot \sin\left(\frac{\pi}{6}\right) \\ -c \\ -c \cdot \sin\left(\frac{\pi}{6}\right) \\ -c \cdot \sin\left(\frac{\pi}{6}\right) \\ 0 \end{pmatrix} = \begin{pmatrix} 60.4 \\ -30.2 \\ -30.2 \\ 60.4 \\ -30.2 \\ -30.2 \\ 0.0 \end{pmatrix} \cdot \text{mm}$ <p>$-c := \tan\left(\frac{\pi}{6}\right) \cdot s = 60.39 \text{mm}$</p>	$i=j=1,2,\dots,7$ $\text{GMD}_{i,j} := \sqrt{(XX_i - XX_j)^2 + (YY_i - YY_j)^2}$
--	--

Figure 2 – Illustration of GMD matrix build up

In Figure 2, c is the distance from the core centres to the cable centre and s is the core diameter.

From the geometrical representation of the cable geometry, the Inductance matrix X_m can be calculated for the cable with ground return, similar to the ones set up in Appendix B.7 of Cigre TB 531 [1] but with screens and armour included.

$\text{GMR} := \begin{pmatrix} f_c r_c \\ f_c r_c \\ f_c r_c \\ r_s \\ r_s \\ r_s \\ r_a \end{pmatrix} = \begin{pmatrix} 15.721 \\ 15.721 \\ 15.721 \\ 47.9 \\ 47.9 \\ 47.9 \\ 116 \end{pmatrix} \cdot \text{mm}$ $f_c := c^{-0.25} = 0.8146 \quad D_e = 400 \sqrt{\frac{\rho}{f}}$ <p>$\theta_c = \theta_s = 20^\circ\text{C}$</p>	$X_{m_{i,j}} := \begin{cases} \frac{i\omega \cdot \mu_0 \cdot \mu_r}{2\pi} \cdot \ln\left(\frac{D_e}{\text{GMD}_{i,j}}\right) & \text{if } \text{GMD}_{i,j} > \max(\text{GMR}_i, \text{GMR}_j) \\ \frac{i\omega \cdot \mu_0 \cdot \mu_r}{2\pi} \cdot \ln\left(\frac{D_e}{\max(\text{GMR}_i, \text{GMR}_j)}\right) & \text{if } \text{GMD}_{i,j} \leq \max(\text{GMR}_i, \text{GMR}_j) \end{cases}$ $X_{m_{LF_{i,j}}} := \begin{cases} \text{LF}_{\text{core}} \cdot X_{m_{i,j}} & \text{if } i < 7 \vee j < 7 \\ \text{LF}_a \cdot X_{m_{i,j}} & \text{if } i = 7 \wedge j = 7 \end{cases}$
--	---

Figure 3 – Illustration of GMR and inductance matrix build up

In Figure 3 we have from Table 1, r_c the outer radius of the conductors, r_s and r_a are the mean radii of metallic sheath/ screen and armour, and f_a the factor giving the GMR of a solid conductor adjusted for the skin effect, with y_s from IEC 60287, and TB 531. Using the f_a factor will, in the further calculations, account for the internal inductance of the conductor. Fortunately, utilisation of y_s from IEC 60287/ TB 531 can provide an accurate result in the frequency range we will focus on, without the need for the Bessel function expressions of the internal impedance. X_m is the inductance matrix which is built up by a simple 2 step function based Equ. (5) calculating the inductance with ground return (D_e):

$$X_{ij} = \frac{\omega \mu_0}{2\pi} \ln\left(\frac{D_e}{x}\right) \quad (5)$$

Where; x is the GMR for the conductor for self inductances, x is the GMR of the outer conductor when one conductor is enclosed in another and x is the GMD between the conductors if the conductors are external to each other.

$X_{m_{LF}}$ is a first suggestion for the implementation of the lay length factors on the inductance, applying the armour wire lay factor on the armour self inductance, and the Core Lay factor on all other positions. This may have to be reconsidered at a later stage.

The total Z matrix is subsequently found by adding the resistive part similar to the inductance matrix (as is done in in Appendix B.7 of Cigre TB 531 [3]), and the inverse Z matrix Y is calculated.

$R := \begin{pmatrix} R_{c.ac} \\ R_{c.ac} \\ R_{c.ac} \\ R_s \\ R_s \\ R_s \\ R_a \end{pmatrix} = \begin{pmatrix} 0.02728 \\ 0.02728 \\ 0.02728 \\ 0.24191 \\ 0.24191 \\ 0.24191 \\ 0.27639 \end{pmatrix} \cdot \frac{\text{ohm}}{\text{km}}$	$R_g := \frac{\omega \cdot \mu_0}{8} = 0.049 \frac{\text{ohm}}{\text{km}}$ <p style="text-align: center;">$\theta_c = \theta_s = 20^\circ\text{C}$</p>	$Z_{\text{cable}} := X m_{LF}$ $Z_{\text{cable}_{i,i}} := X m_{LF_{i,i}} + R_i$ $Z_{i,j} := Z_{\text{cable}_{i,j}} + R_g$ $Y := Z^{-1}$
--	---	---

Figure 4 – Illustration of resistance and Z matrix build up

In Figure 4, R is the a.c. resistances vector which is added to the diagonal of the impedance matrix including correction for temperature correction (if any) and lay factors as well as proximity effect and skin effect for the conductors ($R_{c.ac} = R_c$ in Equ. (8)); R_g from Equ. (23) is the resistance of the ground return, added in all positions. Y is the inversed impedance matrix.

The zero sequence impedance, Z_0 , if found from the oriented node-arc graph in Figure 1 describing the circuit, by applying Kirchhoff's and ohms laws on the circuit by means of node incident matrix for oriented graphs as described by Franksen in [9] and [10] also denoted the topology matrix or just the A matrix (see Figure 5) for a system. (A denotes arcs in the rows, nodes in the column(s), 1 for arcs beginning in a node -1 for ending in a node, all 0's for loops, one node/row exclude as origin, here node 0 for distant ground).

The resulting reduction of the circuit is in line with what is done to reduce the impedance matrix e.g. in [6], [8] and [11] by what in [11] is referenced as a “Kron reduction” but in [12] is done more directly on the full inverse Z matrix but without the Graf theoretical bases as with the use of the incident matrix.

$\text{Beg} := \begin{pmatrix} 1 \\ 1 \\ 1 \\ 0 \\ 0 \\ 0 \\ 0 \end{pmatrix} \quad \text{End} := \begin{pmatrix} 0 \\ 0 \\ 0 \\ 0 \\ 0 \\ 0 \\ 0 \end{pmatrix} \quad A_0 = \begin{pmatrix} 1 \\ 1 \\ 1 \\ 0 \\ 0 \\ 0 \\ 0 \end{pmatrix}$ <p style="text-align: center;">$I_0 = 10 \text{ kA}$</p> <p style="text-align: center;">$\theta_c = \theta_s = 20^\circ\text{C}$</p>	$Z_0 := 3 \left(A_0^T \cdot Y \cdot A_0 \right)^{-1} = (0.1818 + 0.0945i) \cdot \frac{\text{ohm}}{\text{km}}$ $V_0 := Z_0 \cdot I_0 = (1.818 + 0.945i) \cdot \frac{\text{kV}}{\text{km}}$ $I_{0,\text{all}} := Y \cdot (A_0 \cdot V_0) = \begin{pmatrix} 10 \\ 10 \\ 10 \\ -7.95 - 1.18i \\ -7.95 - 1.18i \\ -7.95 - 1.18i \\ -5.45 - 0.19i \end{pmatrix} \cdot \text{kA}$ $\sum_i I_{0,\text{all } i} = (0.707 - 3.738i) \text{ kA}$
--	--

Figure 5 – Illustration of Z_0 calculation

In Figure 5, Beg and End are the arc vectors stating the beginning and end node number of each arc, A_0 is the incident node/arc matrix describing the zero sequence circuit as an orientated linear graph. Since there are only 2 nodes in the circuit the zero sequence impedance Z_0 is found directly from the reduction. There is good alignment to the analytical result (0.15 %) but it found to be issue implementing the lay factors, if $LF_a = LF_{\text{core}}$ there is alignment to calculation tool accuracy (10^{-14}). Going further round in the “Roth diagram” even the circulating currents can be found, revealing that almost 20 % of the current returns in the armour and the ground return current can be calculated. I_0 of 10 kA is a sample current for illustration only.

To calculate the positive sequence impedance it is possible to reuse the setup of the Y matrix (Z^{-1}) (but now at operating temperature) we can also calculate the phase matrix by creating a new incident matrix for a system with 4 nodes since node 1 in Figure 1 is split into 3 so the 3 phase currents can be applied to the phases. The eddy current should now be included as well.

$\text{Beg} := \begin{pmatrix} 1 \\ 2 \\ 3 \\ 0 \\ 0 \\ 0 \\ 0 \end{pmatrix} \quad \text{End} := \begin{pmatrix} 0 \\ 0 \\ 0 \\ 0 \\ 0 \\ 0 \\ 0 \end{pmatrix} \quad \text{_A} = \begin{pmatrix} 1 & 0 & 0 \\ 0 & 1 & 0 \\ 0 & 0 & 1 \\ 0 & 0 & 0 \\ 0 & 0 & 0 \\ 0 & 0 & 0 \\ 0 & 0 & 0 \end{pmatrix} \quad I_1 := 1000\text{A} \begin{pmatrix} 1 \\ a \\ 2 \end{pmatrix}$ $\text{_A}_{i,j} := (j = \text{Beg}_i) - (j = \text{End}_i) \quad F \cdot \lambda''_1 := 0.0972$ $Z \text{ updated to } \theta_c=90^\circ \quad \theta_s=72.65^\circ\text{C} \quad \lambda_2 := 0$	$Z_{\text{node}} := [(\text{_A})^T \cdot Y \cdot \text{_A}]^{-1} \quad (\text{or } Z_{\text{phase}})$ $= \begin{pmatrix} 0.095 + 0.114i & 0.058 - 5.283i \times 10^{-3} & 0.058 - 5.283i \times 10^{-3} \\ 0.058 - 5.283i \times 10^{-3} & 0.095 + 0.114i & 0.058 - 5.283i \times 10^{-3} \\ 0.058 - 5.283i \times 10^{-3} & 0.058 - 5.283i \times 10^{-3} & 0.095 + 0.114i \end{pmatrix} \frac{\text{ohm}}{\text{km}}$ $V_1 := Z_{\text{node}} \cdot I_1 = \begin{pmatrix} 37.056 + 119.322i \\ 84.808 - 91.752i \\ -121.864 - 27.569i \end{pmatrix} \cdot \frac{\text{V}}{\text{km}}$ $I_{1,\text{all}} := Y(\text{_A} \cdot V_1) = \begin{pmatrix} 1000 \\ -500 - 866i \\ -500 + 866i \\ -40.4 - 197i \\ -150.4 + 133.5i \\ 190.8 + 63.5i \\ -0 - 0i \end{pmatrix} \text{A}$ $Z'_{1j} := \frac{V_{1j}}{I_{1j}} = \begin{pmatrix} 0.03706 + 0.11932i \\ 0.03706 + 0.11932i \\ 0.03706 + 0.11932i \end{pmatrix} \frac{\text{ohm}}{\text{km}}$ $Z_1 := Z'_{1j} + R_{c,\text{ac}} \cdot (F \cdot \lambda''_1 + \lambda_2) = (0.039707 + 0.119322i) \frac{\text{ohm}}{\text{km}}$
--	--

Figure 6 – Illustration of Z_1 calculation

In Figure 6, *Beg* is now showing the 3 nodes of the end 3 phase conductors. This time a sample phase current is applied to give the positive sequence impedance and the eddy current is added since it is decided in Cigre WG B1.56 [3] to include it even for both end bonded systems. The current matrix I_1 shows that there is no current in the armour, so the assumption in CIGRE TB 531 simplified analytical calculation that the armour can be neglected for circulating currents are of course correct for the positive sequence impedance, but armour losses from the rating calculations should be included for magnetic armour.

To check the CIM method credibility, the sequence impedance calculated using the simplified analytical Cigre TB 531 table 12 formulas [1] using the values already calculated for the Z matrix above.

$\text{_Z}_a := Z_{1,1} \quad \text{_Z}_m := Z_{1,4}$ $\text{_Z}_x := Z_{1,2} \quad \text{_X}_a := X_{mLF1,1}$ $\text{_Z}_s := Z_{4,4}$	$Z_{1,\text{TB531}} := (\text{_Z}_a - \text{_Z}_x) - \frac{(\text{_Z}_m - \text{_Z}_x)^2}{\text{_Z}_s - \text{_Z}_x} + R_{c,\text{ac}} \cdot F \cdot \lambda''_1 = (0.039707 + 0.119322i) \frac{\text{ohm}}{\text{km}}$ <p>@ $\theta_c=90^\circ \quad \theta_s=72.65^\circ\text{C} \quad F \cdot \lambda''_1 := 0.0972$</p> $Z_{0,\text{TB531}} := LF_{\text{core}} \cdot R_{\text{dc}} \cdot (1 + y_s) + i \cdot \text{_X}_a + 2 \cdot \text{_Z}_x - \frac{(\text{_Z}_m + 2 \cdot \text{_Z}_x)^2}{\text{_Z}_s + 2 \cdot \text{_Z}_x} = (0.1639 + 0.1005i) \frac{\text{ohm}}{\text{km}}$ <p>@ $\theta_c = \theta_s = 20^\circ\text{C}$</p>
--	--

Figure 7 – Cigre TB 531 analytical calculation comparison

From Figure 7, it can be seen that the CIM method gives perfect agreement (Calculation tool accuracy) to the Cigre TB 531 analytical calculation for power frequency positive sequence impedance calculation on the selected submarine 3-core submarine cable design as long as eddy currents λ''_1 (from WG B1.56 [3]) are either included or not included in both calculations and that proximity and skin effect is included in the resistive part of the conductor self impedance. But since the armour is not included in the zero sequence impedance in TB 531 there is as expected some deviation. 11% on resistance, 7% on the inductance, more deviations are of course expected for Submarine cables with aluminium or magnetic steel armour as e.g. reported in [13].

2.2 New analytical method proposed

2.2.1 Method development

At present, modern 3-core HVAC submarine cable design are mostly of separate lead (SL) or separate aluminium (SA) sheath type with common protective single-layer wire armour. The armour material can be either magnetic (e.g. galvanised steel) or non-magnetic (e.g. stainless steel, aluminium) and sometimes, in wet cable designs, the metallic sheath is replaced with metallic wire screen.

Therefore, the newly proposed analytical sequence impedance calculation method is specifically developed for the modern submarine designs described above. Its applicability towards alternative submarine designs is discussed in Chapter 3.

Positive/ negative sequence impedance

For the positive/ negative sequence impedance calculation under balanced three phase currents, current return paths are not considered. Thus, the equivalent three-phase circuit can be simplified as single-phase circuit due to circuit symmetry and electrical first principles can be applied directly.

Therefore, the 3-core submarine cable positive sequence, Z_1 , can be defined as

$$Z_1 = R_1 + jX_1 \quad (6)$$

Where; the positive sequence resistance, R_1 , shall reflect and include associated cable conductor loss, cable screen/ sheath loss, and cable armour loss. Similarly, the positive sequence inductive reactance, X_1 , shall reflect and include associated cable conductor internal self inductance, mutual inductance between conductor and cable screen/ sheath of the same cable core, and mutual inductance between cable screens/ sheaths from different cores.

Note that the inductance between the cable conductor of one core and cable screen/ sheath of another core is considered negligible due to the screening effect from the same-core cable screen/ sheath enclosing the cable conductor. Also, any inductance related to the cable armour and other earth return paths (e.g. seabed, seawater) is considered negligible compared with other main inductance contributors because only little or no induced armour circulating current or ground return current is expected under balanced conductor currents injection due to phase cancellation effect and metallic screen/ sheath shielding effect.

The analytical formulae for the parameters in Equ. (6) are detailed in Section 2.2.2.

Zero sequence impedance

For the zero sequence impedance, the submarine cable under constant three-phase conductor currents injection is described in Figure 8 assuming both end cable system bonding.

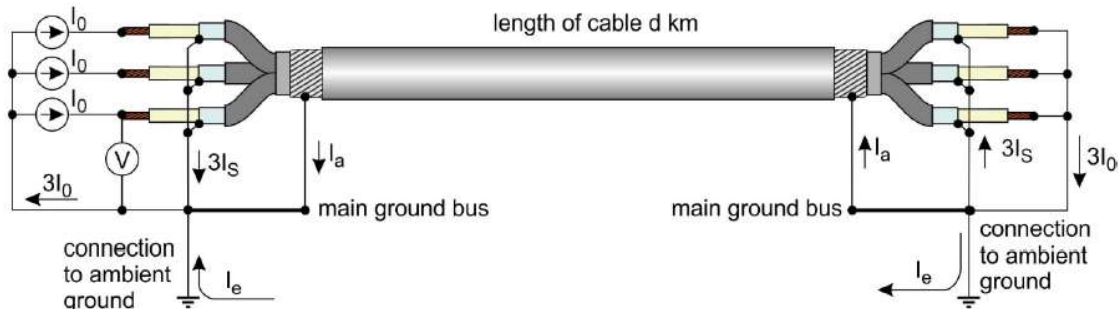


Figure 8 – Illustrative cable connection

In Figure 8, zero sequence current, I_0 , is injected into the 3x phase conductors with return paths through cable metallic screen/sheath, $3I_s$, cable armour, I_a , and remote ground, I_e , in parallel. Note that the factor 3 is included for certain paths due to the fact that there are 3x outgoing conductors, 3x return metallic screen/sheath paths, 1x return armour path, and 1x return remote ground path from a 3-core SA/ SL type submarine cable system.

To draw an equivalent circuit from the illustrative cable connection, following assumptions and simplifications (A&S) have been made.

- I. For SA/ SL type cable, the metallic sheath is normally a thin shell (2 – 3mm), thus its self-inductance is assumed negligible, in [12] critical frequency f_c for 5 mm lead is calculated to 5 kHz (100 harmonics). Similarly, although the stainless steel (non-magnetic) armour wire

thickness can reach 4 – 6 mm it still can be considered thin. However, the armour self-flux linkage will be much weaker than cable phase conductor due the circumferential wire distribution (contrary to conductor strands deployment). Therefore, the self-inductance of the wired armour layer is also assumed negligible.

- II. For SA/ SL type cable, the sheath-sheath mutual inductance under zero sequence impedance shall be negligible because the net flux linkage between any two sheaths loop shall be zero considering 3x identical conductor current vector in trefoil positions.
- III. For the remote ground return path, the ‘Infinite Sea Model’ is used to represent it as a dimensionless conductor with certain resistance at a certain distance, therefore its self-inductance is also neglected.
- IV. The mutual inductance between two objects, e.g. a and b, shall be equal, i.e. $M_{ab} = M_{ba}$, and the resulting induced emf/ current shall give counter effect to the original current based on Lenz law. To avoid an infinite loop feedback of counter effect (e.g. induced current on object B from current in A creates field countering A field and reduces the overall current on A, and the overall reduced A current then leads to a smaller induced B current, and so on...), the mutual inductance is only applied to one of the two objects interacting with each other. All the subsequent loop feedbacks are ignored to simplify the circuit build up which means the assigned mutual inductance value is expected to be slightly higher than reality.
- V. Due to the possible layer shielding effect considering concentric layer positions, mutual inductances are only respectively considered between core conductor – same core metallic sheath (Loop 1), metallic sheath – common armour (Loop 2), and common armour – remote ground earth return (Loop 3). For instance, direct mutual inductance between core conductor and common armour is covered indirectly through these loops as is also used in the Schelknoff model described in Cigre B531.

Based on above assumptions and simplifications, the equivalent electric circuit is drawn and presented in Figure 9 below for the submarine cable zero sequence impedance calculations.

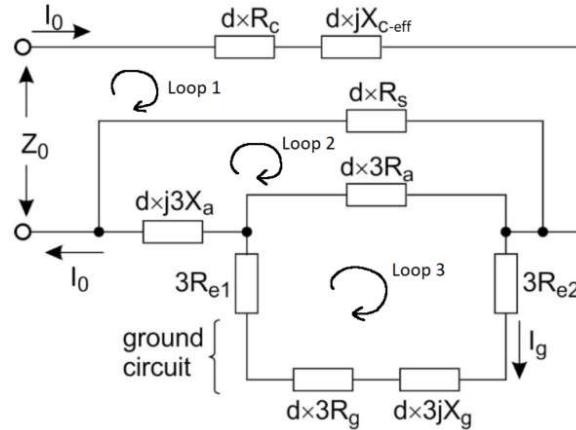


Figure 9 – Equivalent circuit for zero sequence impedance calculation

Where; R_c , R_s , R_a , R_g , are the per unit length a.c. electrical resistance of conductor, metallic screen/ sheath, armour, and remote ground return, X_{c-eff} is the effective conductor inductive reactance consisting of conductor internal inductance and conductor-sheath mutual inductive reactance, X_a is the sheath-armour mutual inductive reactance, X_g is the armour-remote ground return mutual inductive reactance, and R_{e1} , R_{e2} are the two sheath grounding resistances at either cable connection end.

Note that for the equivalent circuit in Figure 9, the sheath inductive reactance X_s is not included because its self-inductance and mutual inductance against other sheath are ignored based on A&S I and II, and

its mutual inductances against core conductor and armour layer respectively have been presented and included in conductor inductive reactance X_{c-eff} and armour inductive reactance X_a based on A&S IV.

The armour inductive reactance X_a doesn't include armour self-inductance based on A&S II, and it only presents the magnetic interaction between metallic sheath and armour based on A&S IV.

The magnetic interaction between armour and remote earth return is represented by ground inductive reactance X_g based on A&S IV, and the ground inductive reactance X_g doesn't include the ground return path self-inductance based on A&S III.

Due to the cascade/shield effect from A&S V, the respective magnetic interaction loop between conductor and sheath (Loop 1), between sheath and armour (Loop 2), and between armour and the remote earth return (Loop 3) shall not magnetically directly interfere with one another. In addition, A&S IV requires only one mutual inductance exist within each magnetic interaction loop.

The grounding resistances, R_{e1} and R_{e2} , are normally small compared to other impedances in the circuit diagram and thus can be neglected.

The analytical formulae for the parameters in the Figure 9 equivalent circuit are detailed in Section 2.2.2.

2.2.2 Analytical formulae

Following the sequence impedance calculation methods proposed in Section 2.2.1, supplementary analytical formulae are introduced in this section. To simplify its application for a wider user group, existing industrial ballpark cable design calculations (e.g. a.c. resistance, loss factor, etc.) are referenced as much as possible. However, a balance evaluation between formulae complexity and required calculation accuracy is always recommended, as per further discussed in Chapter 3.

For the positive/ negative sequence impedance, Z_I , calculation under power frequencies, following analytical formulae are proposed.

$$R_1 = R_c[1 + \lambda'_1 + \lambda''_1 + \lambda_2] \quad (7)$$

$$R_c = LF_{core} \cdot R_{dc}[1 + F_a(y_s + F_{m-shield} \cdot y_p)] \quad (8)$$

$$X_1 = LF_{core} \cdot [\omega L_{c-int} + F_{m-enhance}(\omega L_{cs} + \omega L_{ss})] \quad (9)$$

$$LF = \sqrt{1 + \left[\frac{\pi \cdot \text{lay_diameter}}{\text{Lengt_of_lay}} \right]^2} \quad (10)$$

$$L_{c-int} = \frac{\mu_0}{8\pi(1+y_s)} \quad (11)$$

$$L_{cs} = \frac{\mu_0}{2\pi} \ln\left(\frac{d}{d_c}\right) \quad (12)$$

$$L_{ss} = F_{m-shield} \cdot \frac{\mu_0}{2\pi} \ln\left(\frac{2s}{d}\right) \quad (13)$$

$$\omega = 2\pi f \quad (14)$$

$$F_{m-shield} = 1 - \frac{R_c}{R_s} \lambda'_1 \quad (15)$$

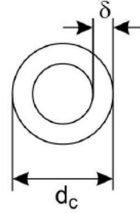
Where; R_I is the positive sequence resistance per unit length of the cable, R_{dc} is the conductor dc resistance per unit length of the cable core at specific temperature, R_c is the conductor a.c. resistance per unit length of the cable at specific temperature, F_a is conductor resistance enhance factor due to the

presence of magnetic armour, μ_0 is the absolute permeability of the free space, $F_{m-shield}$ is the magnetic field shielding factor due to the screening effect from the core metallic screen/ sheath, $F_{m-enhance}$ is the magnetic field enhancement factor for air medium inside the cable due to the presence of magnetic armour, L_{c-int} is the conductor internal self inductance per unit length of cable core, L_{cs} is the conductor-sheath/screen mutual inductance of the same core per unit length of cable core, L_{ss} is the inter-core sheath-sheath mutual inductance per unit length of cable core, f is the operating frequency, LF is the lay length factor due to stranding mechanism as per detailed in Cigre WG B1.56 recommendations [3], and LF_{core} is the cable core lay length factor. All other parameters are defined and calculated as per [4] and IEC 60287-1-1 [2].

The magnetic field shielding effect factor, $F_{m-shield}$, is introduced to represent the core sheath/ screen shielding effect on conductor resistance proximity effect, y_p , and sheath-sheath mutual inductance, L_{ss} , taking the expression similar to the approach from IEC 60287-1-1 section 2.4.2.5. A further discussion of this factor is included in Section 3.1.

The cable conductor internal self inductance, L_{c-int} , is generally considered constant, $\mu_0/8\pi$, under power frequencies [4]. However, for a more accurate calculation taking into account the conductor skin effect (i.e. limiting the conductor internal flux linkage area to within the skin depth as the current is pushed towards outer radii), the Equ. (11) is derived as follows,

Considering a frequency dependant skin depth, δ , and a conductor outer diameter, d_c , the skin effect ratio [4], k_{sk} , of conductor resistance with skin effect to that without becomes,



$$\frac{R_{sk}}{R} = k_{sk} = 1 + y_s \approx \frac{\frac{\rho}{\pi \cdot d_c \cdot \delta}}{\frac{\rho}{\pi \cdot \left(\frac{d_c}{2}\right)^2}} = \frac{d_c}{4 \cdot \delta} \quad (16)$$

$$\delta = \frac{d_c}{4 \cdot (1 + y_s)} \quad (17)$$

Therefore, as the conductor internal self inductance is proportional to the flux linkage area, the reduced L_{c-int} at higher frequencies becomes,

$$L_{c-int} \approx \frac{\mu_0}{8\pi} \cdot \frac{\pi \cdot d_c \cdot \delta}{\pi \cdot \left(\frac{d_c}{2}\right)^2} = \frac{\mu_0}{8\pi(1+y_s)} \quad (18)$$

Note that $F_a = 1.0$ and $F_{m-enhance} = 1.0$ for submarine cables with non-magnetic armour and a ballpark value of $LF_{core} = 1.01$ may be used based on manufacturer experience [3].

The calculation of conductor dc resistance R_{dc} , sheath loss factor λ_1 , armour loss factor λ_2 , conductor resistance enhancement factor F_a , overall inductive reactance X_l , and relative permeability μ_r is further discussed in Chapter 3 as they may impact the calculation accuracy.

For the zero sequence impedance, Z_0 , calculation under power frequencies, following analytical formulae are proposed based on the Figure 9 equivalent circuit [14].

$$Z_0 = R_0 + jX_0 = R_c + j \cdot X_{c-eff} + \frac{3R_s \left[j \cdot X_a + \frac{R_a(R_g + j \cdot X_g)}{R_a + R_g + j \cdot X_g} \right]}{R_s + 3j \cdot X_a + \frac{3R_a(R_g + j \cdot X_g)}{R_a + R_g + j \cdot X_g}} \quad (19)$$

$$R_0 \approx R_c + Re \left\{ \left[j \cdot X_a + \frac{R_a(R_g + j \cdot X_g)}{R_a + R_g + j \cdot X_g} \right] \cdot \frac{3R_s}{R_s + 3j \cdot X_a + \frac{3R_a(R_g + j \cdot X_g)}{R_a + R_g + j \cdot X_g}} \right\} \quad (20)$$

$$X_0 = X_{c-eff} + Im \left\{ \left[j \cdot X_a + \frac{R_a(R_g + j \cdot X_g)}{R_a + R_g + j \cdot X_g} \right] \cdot \frac{3R_s}{R_s + 3j \cdot X_a + \frac{3R_a(R_g + j \cdot X_g)}{R_a + R_g + j \cdot X_g}} \right\} \quad (21)$$

$$X_{c-eff} = LF_{core} \cdot (\omega L_{c-int} + F_{m-enhance} \cdot \omega L_{cs}) \quad (22)$$

$$R_g = \frac{\omega \mu_0}{8} \quad (23)$$

$$X_g = LF_a \cdot \frac{\omega \mu_0}{2\pi} \ln \left(\frac{D_e}{r_a} \right) \quad (24)$$

$$X_a = F_{m-enhance} \cdot LF_{core} \cdot \frac{\omega \mu_0}{2\pi} \ln \left(\frac{r_a}{\sqrt[3]{s^2 r_s}} \right) \quad (25)$$

$$D_e = 400 \sqrt{\frac{\rho}{f}} \quad (26)$$

Where; ρ is the seawater electrical resistivity (normally 0.2 – 1.0 $\Omega \cdot m$) used for the ‘Infinite Sea Model’ [1], r_s is the mean sheath/ screen radius, r_a is the mean armour layer radius, D_e is the equivalent earth return path depth, R_g is the equivalent earth return per unit length electrical resistance, R_s is the a.c. resistance of cable sheath/ screen at specific temperature per unit length of cable, R_a is the a.c. resistance of cable armour at specific temperature per unit length of cable, and LF_a is the cable armour wire lay length factor. All other parameters are defined and calculated as per [3] and [2].

Note that $F_{m-enhance} = 1.0$ for submarine cables with non-magnetic armour and a ballpark value of $LF_{core} = 1.01$ may be used based on manufacturer experience [3].

The calculation of sheath-armour inductive reactance X_a , armour-ground inductive reactance X_g , effective conductor inductive reactance X_{c-eff} , and magnetic field enhancement factor $F_{m-enhance}$ is further discussed in Chapter 3 as they may impact the calculation accuracy.

2.3 Analytical method application and benchmarking

2.3.1 Sample step-by-step calculation

The cable design under the sample calculation is taken from case 8 of [3], which is a 220 kV 3-core SL type submarine cable with 1000 mm² Cu conductor and stainless steel armouring.

Some parameters are temperature dependent and therefore the operating temperature conditions in [3] are reproduced here, i.e. $\theta_{conductor} = 90^\circ C$, $\theta_{sheat} = 72.65^\circ C$ and $\theta_{armour} = 68.52^\circ C$ as high temperature condition, and $\theta_{conductor} = \theta_{sheat} = \theta_{armour} = 20^\circ C$ as low temperature condition. The calculations are performed for 50 Hz power frequency.

All required input parameters are presented in Table 1, and positive/negative sequence impedance and zero impedance calculation results are presented in Table 2 and Table 3 respectively.

Table 1. Input parameters for the example calculations

Parameter	Value	Unit	Reference
R_{dc} (@90°C)	0.0224	Ω/km of core	Cable datasheet
y_s	0.1444	-	[3]
y_p	0.0568	-	[3]
$lay_diameter$	$1.29 \cdot s = 134.934$	Mm	[3]
LF_a	1.0311	-	Cable datasheet/ Equ. (9)
F_a	1.0	-	Stainless
$F_{m-enhance}$	1.0	-	Stainless
λ'_1	0.3585	-	[3]
λ''_1	0.0972	-	[3]
λ_2	0	-	[3]
r_c	19.3	Mm	Cable datasheet
r_s	47.9	Mm	Cable datasheet
r_a	116	Mm	Cable datasheet
s	104.6	Mm	Cable datasheet
f	50	Hz	Power frequency
R_s (@20°C)	0.1975	Ω/km of cable	[3]
R_s (@72.65°C)	0.2419	Ω/km of cable	[3]
R_a (@20°C)	0.2764	Ω/km of cable	[3]
ρ	1.0	$\Omega \cdot \text{m}$	Specific site data

Table 2. Positive sequence impedance for the example case at high temperature condition

Parameter	Value	Unit	Reference
LF_{core}	1.0118	-	Equ. (10)
$F_{m-shield}$	0.9596	-	Equ. (15)
R_c	0.0272	Ω/km of cable	Equ. (8)
R_1	0.0397	Ω/km of cable	Equ. (7)
L_{c-int}	0.0437	mH/km	Equ. (11)
L_{cs}	0.1818	mH/km	Equ. (12)
L_{ss}	0.1499	mH/km	Equ. (13)
X_1	0.1193	Ω/km of cable	Equ. (9)
Z_1	$0.0397 + 0.1193j$	Ω/km of cable	Equ. (6)

Table 3. Zero sequence impedance for the example case at low temperature condition

Parameter	Value	Unit	Reference
R_g	0.0493	Ω/km	Equ. (23)
D_e	56.5685	m	Equ. (26)
X_{c-eff}	0.0708	Ω/km of cable	Equ. (22)
X_g	0.4010	Ω/km of cable	Equ. (24)
X_a	0.0231	Ω/km of cable	Equ. (25)
R_0	0.1819	Ω/km of cable	Equ. (20)
X_0	0.0934	Ω/km of cable	Equ. (21)
Z_0	$0.1819 + 0.0934j$	Ω/km of cable	Equ. (19)

2.3.2 Calculation results benchmarking

In this Section, the analytical sequence impedance calculation results from the preceding Section have been compared with the results from the alternative CIM method and finite element analysis (FEA) respectively on the same cable design and operation condition(s). Considering the CIM method has been detailed in Section 2.1.2, only a short description of FEA is given below.

The FEA calculation has been performed on the 3D cable geometry using the commercial package COMSOL Multiphysics© [15]. To optimise the computation time, the model geometry consists of a thin slice of the cable, where periodic boundary conditions are applied at both sides of the cable to account for the effect of the core and armour axial stranding [16] [17].

The inputs for the FEA model are the geometry parameters and material properties specified in [3], and the resistivity of the surrounding environment is considered $\rho = 1 \Omega.m$, as in the analytical calculation.

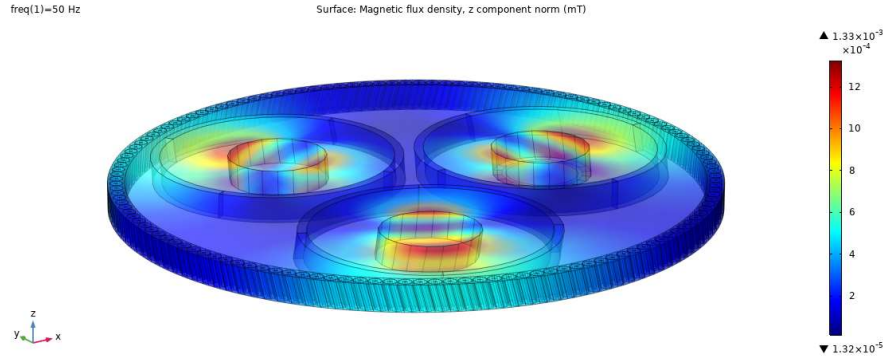


Figure 10 – 3D cable model for Z_1 calculation at 50 Hz Magnetic flux density plot under 1A three-phase balanced conductor currents

The calculation of the Z_1 is done by injecting a current equal in magnitude and 120° out of phase to the cable cores, and assigning a voltage equal to zero to the sheaths and armour. The output of the FEM calculation is the impedance of each core, which corresponds the voltage drop along the core divided by the injected current, and takes into account the self-inductance of each conductive elements and mutual inductance between all the conductive elements. The calculation of the Z_0 follows a similar procedure, by injecting a current equal in magnitude and phase to the cable conductors, and assigning a voltage equal to zero to the sheath and armour.

Table 4 and Table 5 present the comparison of the Z_1 and Z_0 results from the analytical calculation and alternative methods for the example case, at the same operation conditions.

Table 4. Comparison of Z_1 results of 50 Hz and at high temperature

Parameter	Analytical results [Ω/km]	FEA results [Ω/km]	CIM/ TB531* results [Ω/km]	Variation [%]
Z_1	0.0397+0.1193j	0.0390+0.1184j	0.0397+0.1193j	
R_1	0.0397	0.0390	0.0397	-1.8 / 0
X_1	0.1193	0.1184	0.1193	-0.8 / 0

*TB 531 modified with eddy currents and including effect of y_p and y_s on R_c and y_s on $X(f_c r_c)$.

Table 5. Comparison of Z_0 results of 50 Hz and at low temperature

Parameter	Analytical results [Ω/km]	FEA results [Ω/km]	CIM results [Ω/km]	TB531 results [Ω/km]	Variation [%]
Z_0	0.1819+0.0934j	0.1831+0.0954j	0.1818+0.0945j	0.1639+ 0.1193j	
R_0	0.1819	0.1831	0.1818	0.1639	0.7 / -0.15* /-11
X_0	0.0934	0.0954	0.0945	0.1005	2.1 / 1.1* / 7.1

* known issue with implementation of Lay Factors on inductances, if $LF_a=LF_{core}$ is used there is perfect alignment between Analytical and CIM results.

3. Application Recommendation and Future Work

Considering all the analytical formulae in Section 2.2.2 were originally developed for 3-core submarine cable with non-magnetic armour, as the mostly common export cable design nowadays, under power frequency operations and lots of supplementary equations are taken from IEC 60287-1-1, its calculation accuracy may be affected when the cable design and operating condition deviate from the original case.

3.1 Application recommendation

Physical stranding of submarine cable components

In practical manufacturing of 3-core submarine cables, cable component stranding is necessary to enhance mechanical robustness and stability. Its impacts on cable electrical parameters needs to be considered and addressed properly. Following application recommendation are therefore drawn,

- When stranded conductor is designed, the helical laying characteristics of the conductor strands shall be considered in the R_{dc} calculation. Relevant guideline can be found in [3].
- The stranding effects of cable core, cable metallic screen wire, and cable armour wire on electrical resistance are partially addressed in Section 2.2.2. to update values to a common per unit cable length basis. If the R_{dc} value is either directly measured from complete cable or quoted from IEC 60228 as per unit cable length, the LF_{core} in Equ. (3) shall be removed. When calculating parameters λ_1' , λ_1'' , λ_2 , R_s , and R_a through IEC 60287-1-1 formulae, appropriate lay factors shall be applied as per suggested in [3].
- Although one example in [3] applies cable core lay factor to overall metallic sheath/screen inductance, it is not still clear at this point of time how the stranding mechanism would impact various inductance calculation in a per unit cable length based system, considering most inductance calculation formulae assume straight conductor(s) in parallel. For instance, it can be non-trivial to accurately calculate the mutual inductance between metallic screen wire layer of one lay length and armour wire layer of a different lay length. Following a similar strategy as per [3], cable core lay factor, LF_{core} , has been applied to conductor internal self inductance, conductor-sheath mutual inductance, sheath-sheath mutual inductance, and sheath(s)-armour mutual inductance. Armour wire lay factor, LF_a , has been applied to armour-ground mutual inductance. A further study on this aspect is recommended.

Non-magnetic armour and magnetic armour

For most export submarine cable designs with stainless steel armour, the armour loss is considered negligible (i.e. $\lambda_2 = 0$), there is no additional influence on various inductance calculation inside the cable (i.e. $F_{m-enhance} = 1.0$), and there is no conductor a.c. resistance or screen loss enhancement as mentioned in [3][4].

When magnetic armour is used (most array submarine cables), following application recommendations are drawn,

- Due to a strong skin effect of magnetic armour, an enhancement factor, F_{dc-ac} , between armour dc resistance and a.c. resistance shall be used. A factor value between 1.2 and 1.4 may be used as per IEC 60287-1-1 recommendation. However, for non-magnetic armour, $F_{dc-ac} \approx 1.0$ is recommended based on comparison against FEA modelling.
- The armour loss factor λ_2 is no longer negligible and it shall ideally include armour hysteresis loss and eddy current loss. IEC 60287-1-1 formula may be used but would overestimate the loss factor. It is recommended to align with Cigre WG B1.64 development work and update once concluded.

- The cable conductor a.c. resistance may increase due to the presence of magnetic armour similar to pipe-type cables where $F_a = 1.5$ as per section 2.1.5 of [2]. However, it is recommended to refine this factor through comparison against practical measurement or FEA modelling.
- Due to the presence of the magnetic armour, the air medium enclosed by the armour layer may have a higher effective permeability due to magnetic field compaction which could impact the mutual inductance calculation. The concept has been considered in IEC 60287-1-1 on SL/SA type cable sheath loss factor calculation of adopting the 1.5 enhancement factor. Therefore, a similar field enhancement factor, $F_{m-enhance}$, may be assigned. However, the general value of such parameter is not available at the moment and its quantification could be empirical and require comparison against practical measurement or FEA modelling.

Higher frequencies application

For system harmonics analysis, submarine cable positive/ negative sequence impedance at higher frequencies (up to 5000 to 6000 Hz) may be required. Although IEC 60287-1-1 is not intrinsically created for higher frequencies, following application recommendations are proposed to utilise existing formulae as much as possible.

- All existing IEC 60287-1-1 formulae involving frequency components may still be used at higher frequencies by simply updating parameter f and ω .
- The sheath magnetic field shielding effect factor, $F_{m-shield}$, adopts a similar approach as per IEC 60287-1-1 section 2.4.2.5 and is expected to become stronger as operating frequency increases under Lenz's Law. The physical interpretation of its application to sheath-sheath mutual inductance, L_{ss} , is that when the frequency increases, the induced sheath current will eventually mirror the conductor current of the same core but in opposite direction. Under a balanced loading assumption and symmetrical sheath positions, the overall flux linkage between any two sheaths due to the three sheath currents would approach zero under phase cancelling, leading to a reduction in sheath-sheath mutual inductance.

However, for submarine cables with magnetic armour, this shielding factor can become negative mathematically beyond a particular high frequency value due to an empirical 1.5 factor in the λ_l' formula (section 2.3.10 of [2]). To interpret it through physics perspective, it implies that the proximity effect factor is reduced to negligible beyond that frequency. Considering the factor 1.5 in λ_l' is kind of empirical from specific pipe type cable measurement, one may reduce it to 1.2 or even 1.0 so that it still represents the correct physics expectation as frequency increases but also mathematically valid over the high frequency ranges under study.

For information, a comparison between the proposed analytical method implementing above application recommendations and FEA modelling has been carried out at high frequencies on the same cable design with results being outlined below.

Table 6. Comparison of Z_1 results of high frequencies and at high temperature

Frequencies [Hz]	Analytical results [Ω/km]	FEA results [Ω/km]	R_1 Variation [%]	X_1 Variation [%]
50	0.0397+0.1193j	0.0390+0.1184j	-1.8	-0.8
200	0.145+0.3825j	0.1390+0.3662j	-4.1	-4.3
500	0.263+0.7277j	0.2409+0.7157j	-8.4	-1.6
1000	0.32+1.2906j	0.3141+1.2794j	-1.8	-0.9
2000	0.365+2.4549j	0.3916+2.3964j	7.3	-2.4
5000	0.4378+5.9746j	0.4838+5.7391j	10.5	-3.9

According to the design experience from an offshore wind developer, a positive sequence impedance value uncertainty up to circa. 10% is considered acceptable for system study, compared with a much bigger discrepancy observed between Cigre TB 531 analytical method and some commercial system study packages (e.g. PSCAD).

3.2 Further development

Based on all presented in preceding sections, several further development actions are suggested to further increase the accuracy and applicability of the proposed analytical methods.

Although all the FEA modelling results presented in this paper have been cross-checked between authors from both developer and supplier sides through slightly different 3D models, it is recommended to carry out site sequence impedance measurement(s) in the future to validate the FEA modelling as such technique is still very recent for full-scale 3-core cables.

Another piece of future work is to improve the mutual inductance calculation accuracy between two components of different lay lengths, and its implementation in the calculations. It is recommended to start with a sensitivity study of the impact of uncertain mutual inductances on the overall sequence impedance values.

In this paper, we have for the zero sequence impedance calculation throughout, included proximity effect used in the load calculations in IEC 60287 and excluded the eddy current, this because the proximity effect is part of the ac resistance of the conductor. It can however be seen from the side result from the CIM calculations, that there is a 80% screening of both effects for this particular cable design, and it is suspected that the two effects (without screen screening) are larger for zero sequence compared to positive sequence (e.g. a factor $+\sqrt{3}$?), still, for most designs it is expected that the included proximity effect in total is significantly lower than shown, and the excluded eddy current cannot be completely excluded, which will have to be addressed in future works.

Finally, when magnetic armour is used, further work is needed to refine the armour loss factor calculation as suggested previously and such factor shall ideally capture the frequency dependant armour hysteresis losses. Additional future works may involve empirically quantifying the so-called magnetic field enhancement factor, $F_{m-enhance}$.

4. Conclusion

This paper examines existing sequence impedance calculation practice for 3-core submarine cable circuits with magnetic armour and outlines several knowledge gaps and application challenges based on practical project experiences. After a thorough search and review of relevant literatures, an improved analytical calculation method has been developed and proposed to specifically address the identified existing challenges, through a collaboration between offshore windfarm developer and cable supplier. Such method is primarily based on equivalent circuit theory and developed in simplified analytical form for easy application, with its credibility and accuracy being cross-checked against the more complex numerical methods using the complex impedance matrix method combined with the incident matrix to simplify the matrix reduction and prepare for scalability. With a step-by-step calculation guidance and supplementary application recommendations, the authors believe this method can help to bridge existing knowledge gap and be practically beneficial to the cable industry and encourage future work e.g. in a Cigre work group supplementing TB 531.

BIBLIOGRAPHY

- [1] CIGRE Working Group B1.30, "Cable Systems Electrical Characteristics" (Technical Brochure 531 April 2013).
- [2] TC 20 IEC, "Electric cables - Calculation of the current rating - Part 1-1: Current rating equations (100 % load factor) and calculation of losses - General" (IEC 2014).
- [3] CIGRE Working Group B1.56, "Power Cable Rating Examples for Calculation Tool Verficiations" (DRAFT version 19.09.2019).
- [4] G. J. Anders, "RATING OF ELECTRIC POWER CABLES - Ampacity Computations for Transmission, Distribution, and Industrial Applicabtions" (IEEE Press 1997).
- [5] L. Heinhold, "Power Cables and their Application - Part 1 Materials · Construction Criteria for Selection Project Planning Laying and Installation · Accessories Measureing and Testing" (Siemens Aktiengesellschaft 1990).
- [6] R. Benato, M. Forzan, M. Marelli, A. Orini, E. Zaccone, "Harmonic behaviour of HVDC cables" (EEE PES T&D 2021).
- [7] G. Bianco, G. Luoni, "Induced currents and losses in single-core submarine cables" (IEEE Transactions on Power Apparatus and Systems 1976, volume 95 issue 1).
- [8] N. D. Tleis, "Power Systems Modelling and Fault Analysis: Theory and Practice" (Newnes 2007, Chapter 3 Modelling of multi-conductor overhead lines and cables).
- [9] O. I. Franksen, P Falster, "Colligation or the logical inference of interconnection" (Mathematics and Computers in Simulation, March 2000, Volume 52 Issue 1).
- [10] O. I. Franksen, "An operational Formulation of the Electrical Network problem" (Tapir Publishers 1987, pages 15-178).
- [11] W. H. Kersting, R. K. Green, "The Application of Carson's Equation to the Steady-State Analysis of Distribution Feeders" (IEEE/PES Power Systems Conference and Exposition 2011).
- [12] A. Ametani, T. Ohno, N. Nagaoka, "Cable System Transients: Theory, Modelling and simulation" (IEEE, Willy 2015).
- [13] M. T. Arentsen, et al, "MVAC Submarine Cable, Impedance Measurements and Analysis" (UPEC Conference, 2017).
- [14] G. Henning, "ABB High Voltage Cables AB (now NKT HV Cables AB) on Zero sequence impedance of cables" (Internal note, 2005 or earlier).
- [15] Comsol Multiphysics 5.6, "www.comsol.com," [Online].
- [16] Comsol Multiphysics, Cable Tutorial Series Comsol Multiphysics 5.6, Submarine Cable 8 - Inductive Effects 3D.
- [17] J Del-Pino-López, M Hatlo, P Cruz-Romero, "A 3D Parametric Analysis of Three-core Armoured Power Cables Series Impedance" (SEST conference, 2018).
- [18] A. Ametani, N Nagaoka, Y. Baba, T. Ohno, K. Yamabuki, "Power System Transients - Theory and Applications" (CRC Press 2017, Second Edition).